Medium energy gamma rays following radiative capture of 50 MeV polarized protons on ^{11}B

M. Nomachi,* T. Shibata, K. Okada, T. Motobayashi,
F. Ohtani,† and H. Ejiri
Department of Physics and Laboratory of Nuclear Studies, Osaka University, Toyonaka, Osaka, 560 Japan

T. Kishimoto
Department of Physics, Tokyo Institute of Technology, Tokyo, 152 Japan
(Received 24 February 1984)

Medium energy (40–65 MeV) γ rays following radiative capture of 50 MeV polarized protons on ^{11}B were studied for the first time by using a NaI detector ensemble with good energy resolution and small background counts. Discrete γ rays feeding the ground 0^+, 4.44 MeV 2^+, and 9.64 MeV 3^- states, and prominent γ peaks feeding the 19 and 22 MeV excitations region in ^{12}C were identified. The analyzing powers of the radiative capture were found to depend on the microscopic configurations of the final states.

Low and medium energy γ rays following radiative capture reactions have been used extensively to study nuclear properties of single particle and collective motions, for the electromagnetic interaction involved in the reaction is simple and well known. So far, γ rays in the 10–30 MeV region have been studied mainly to investigate the $E1$ giant resonance ($E1$ GR) in terms of the semidirect process[1] through the GR. Radiative capture reactions of low energy protons with $E_p = 10$–30 MeV have been used[2–9] to study the GR.

Medium energy ($E_\gamma > 50$ MeV) radiative capture far beyond the $E1$ GR energy region is interesting in view of a possible nucleon-correlation effect and an electromagnetic strength in the high energy region. A study of the analyzing power of such γ rays using polarized protons is crucial for investigating the spin direction of the nucleon associated with the transition. The main contributions to the medium energy radiative capture reaction are electric-type transitions, the main terms of which have no spin component. Therefore, the analyzing power may directly reflect the spin direction associated with the radiation. So far, the analyzing power of γ rays has been studied in the energy region of less than 45 MeV;[7] however, there has been no study far beyond the $E1$ GR energy region ($E_\gamma > 50$ MeV). Radiative capture feeding the high-lying region is also interesting for studying properties of highly excited states. So far, the radiative proton capture in the $E_p \approx 30$ MeV region has been used to study a possible $E1$ GR excitation on the highly excited states ($E_x \approx 20$ MeV).[7,9] The analyzing power of the γ rays following radiative capture of 50 MeV polarized protons may directly reflect the properties of the highly excited states, because the γ-ray energy is beyond the $E1$ GR energy. This report aims at presenting the analyzing power measurement of medium energy γ rays following radiative capture of 50 MeV polarized protons and at showing the dependence of the analyzing power on the spin direction of the captured proton.

The experimental study of medium energy γ rays is much harder than that of the GR energy region γ rays following radiative capture of low energy protons ($E_p < 30$ MeV). The γ rays have to be detected in the presence of a huge flux of neutrons, and high resolution measurement of medium energy γ rays is hard. Kovash *et al.*[10] have recently measured discrete γ rays following (p,γ) reactions at $E_p = 40$–80 MeV. Anghinolfi *et al.*[11] have also measured γ rays at $E_p = 18$–43 MeV. Recently, we have succeeded in developing a special NaI crystal ensemble called HERMES (high energy gamma radiation measuring system).[12] It gave fairly clean spectra even for 60–70 MeV γ rays following 50–65 MeV proton bombardments.[13,14] The spectrum was much improved in both the energy resolution and the γ-ray separation from neutrons and cosmic rays. Thus, several discrete γ rays were well observed.

The medium energy γ rays from the $(\vec{p},\gamma)$ reaction on ^{11}B were measured by using 50 MeV polarized protons provided by the Osaka University Research Center for Nuclear Physics cyclotron. The beam intensity was around 15–30 nA and the target used was a self-supporting ^{11}B foil with 31 mg/cm^2 thickness and 98.6% isotopic enrichment. The beam polarization was around 70–75%. The 40–65 MeV γ rays were observed at $\theta_{lab} = 40°$, 60°, 80°, and 110° by HERMES. It consists of an 11 in. $\phi \times 11$ in. NaI ensemble and an annular plastic scintillator shield as a Compton suppressor. The NaI ensemble is composed of the 6 in. $\phi \times 11$ in. central NaI with good energy resolution and an 11 in. $\phi \times 11$ in. annular NaI detector divided optically into four segments. The sum of the signals from these NaI detectors gives the total γ-ray energy. Since a major fraction of the γ-ray energy is deposited in the central NaI, the energy resolution of the total system is as good as the central NaI. The overall resolution for 60 MeV γ rays was about $\Delta E/E \approx 3.8\%$, including 1% due to the target thickness. The energy spectrum of the photons escaping from the central NaI was measured by the annular NaI. It decreases exponentially with the increasing energy deposit in the annular NaI. Thus, a Gaussian plus exponential tail is employed as a response function of the detector. Only two percent of the γ rays deposit more than 3 MeV in the annular NaI. Thus, the effect of the low-energy tail of the detector response function is small.

Cosmic-ray muons cross the annular NaI and deposit energy of about 30 MeV. Thus, events triggered by large sig-

nals (> 15 MeV) coming from the central NaI without being accompanied by a signal beyond 8 MeV from the annular NaI were almost free from such cosmic rays. The central NaI gave the good timing signal too, which was essential for measuring the time-of-flight (TOF). The 0.9 m flight path with the overall time resolution of 3.5 nsec was sufficient to separate γ rays from neutrons as shown in Fig. 1.

The event rate of large pulses beyond 14 MeV for the central crystal was less than 10^3 counts/sec. Thus, the pileup of such large pulses is negligible. The counting rate of small pulses below 3 MeV was an order of 3×10^4 counts/sec, and the pileup of these small pulses on the large pulse in the energy region of present concern makes the energy resolution worse. In order to avoid this, any event following another event within 1 μsec was rejected by using fast coincidence, and a fast clear signal cleared an event after 1 μsec if another pulse followed it within 1 μsec. The circuit could resolve up to 20 nsec.

An observed spectrum at $\theta_{lab}=40°$ is shown in Fig. 1. Several discrete γ-ray peaks from the $^{11}B(\vec{p},\gamma)$ reaction are evidently seen in the 50–65 MeV region. They correspond to γ transitions to the ground 0^+, 4.44 MeV 2^+, and 9.64 MeV 3^- states. Two bumps are also seen in the 18.8 and 22.3 MeV excitation energies. Since these excitation energies are above the proton threshold energy, continuum states can be fed. The γ-ray yields for the 18.8 and 22.3 MeV excitation energy bumps have been obtained by subtracting the continuum γ rays underneath the bumps (see dashed line in the Fig. 1), which are obtained by linear extrapolation of the spectrum of the γ rays feeding higher excited states, for lack of a better model for the continuum γ rays. Absolute cross sections and analyzing powers of these two bumps cannot be obtained without knowing the exact continuum γ-ray spectrum. However, the angular dependences of the cross sections and the analyzing powers of the bumps can be compared with each other, because the continuum γ rays underneath the two bumps are obtained so as to have the same angular dependence of the analyzing power. Actually the analyzing power of the γ rays was almost constant in the higher excitation energy region. Angular dependences of the cross sections and the analyzing powers are shown in Figs. 2 and 3.

The observed differential cross sections for γ_a (ground state 0^+) and γ_b (first excited 2^+) at $\theta_{lab}=60°$ are in accord with those interpolated from the previous data[10] at $E_p=40$ and 60 MeV. The angular distributions for the γ_a and γ_b show a similar forward-peaking pattern. The data for the γ_a agree with the calculation given in Refs. 15 and 16 in terms of both the one-body and the two-body direct processes. It is remarkable to find that the angular dependences of the analyzing powers for the γ_a and γ_b are very different from each other (see Figs. 2 and 3). According to random-phase approximation (RPA) calculations,[17–19] the ground state 0^+ and the first excited 2^+ states have large fractions of $p_{3/2}$ and $p_{1/2}$ proton configurations coupled to the ^{11}B ground state, respectively. The analyzing power for the $j_>(p_{3/2})$

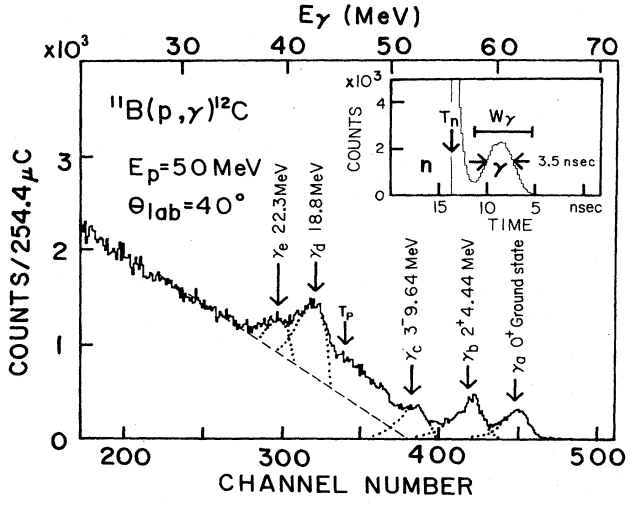

FIG. 1. Gamma-ray energy spectrum for the $^{11}B(p,\gamma)$ reaction. Continuum γ rays underneath the γ_d and γ_e bumps are assumed as the dashed curve. The dotted line is given by a peak fit program. The arrow T_p gives the threshold energy of the proton emission. Inset: A part of the time-of-flight spectrum for the central NaI signals above 15 MeV. Most neutrons with flight time beyond the threshold T_n (see arrow in figure) were not recorded in the on-line data aquisition. Gamma rays in the TOF window $W_\gamma \approx 10$ nsec were selected in the off-line data analysis. The FWHM of 3.5 nsec includes the 2.6 nsec beam width.

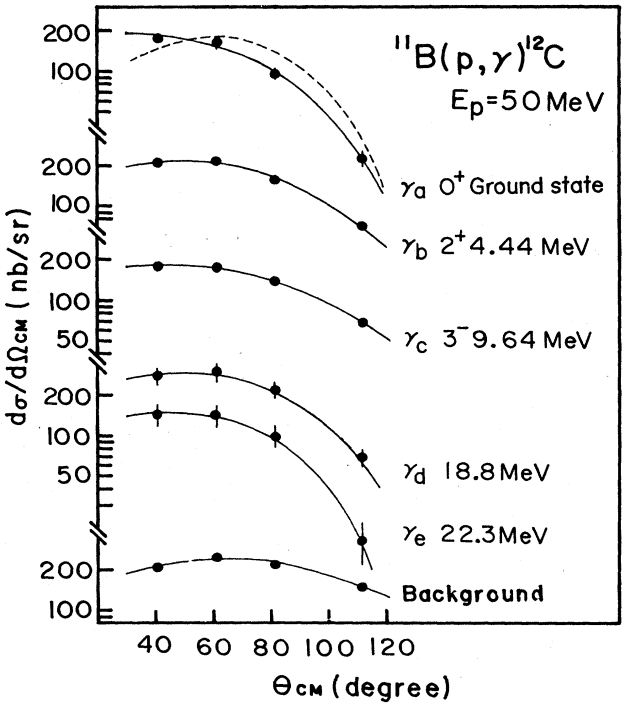

FIG. 2. Differential cross sections for the radiative capture of the 50 MeV polarized protons on ^{11}B. The background in the figure means the continuum γ rays (see Fig. 1) at excitation energy of 19–21 MeV. The solid line shows a Legendre fitting. Legendre expansion coefficients for γ_a are $a_1=1.53\pm0.12$, $a_2=0.57\pm0.08$, those for γ_b are $a_1=0.98\pm0.03$, $a_2=-0.12\pm0.06$, and those for γ_c are $a_1=0.97\pm0.08$, $a_2=-0.15\pm0.08$. The dashed line shows the calculated value, where the angular distribution in Ref. 16 is normalized to the calculated value in Ref. 15. Error bars given are due to ambiguity in evaluating the γ-peak area by using various peak-fitting functions. The systematic error for the absolute cross sections due to the target thickness, the efficiency of the HERMES, and the beam current integration amounts to about 25%.

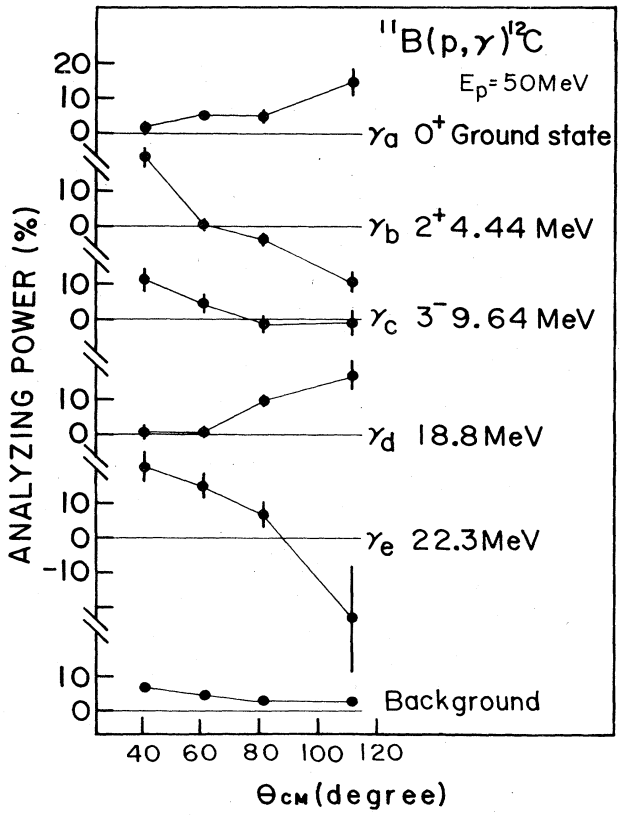

FIG. 3. Analyzing powers $A(\theta)$ for the radiative capture of the 50 MeV polarized protons on ^{11}B. The $A(\theta)$ is defined as $[d\sigma_\uparrow(\theta)/d\Omega - d\sigma_\downarrow(\theta)/d\Omega]/[d\sigma_\uparrow(\theta)/d\Omega + d\sigma_\downarrow(\theta)/d\Omega]$, where $d\sigma_\uparrow/d\Omega$ ($d\sigma_\downarrow/d\Omega$) are the differential cross sections for protons with spin up (spin down) with respect to the axis $\vec{k}_p \times \vec{k}_\gamma$. Solid lines are just to guide eyes. Statistical errors are shown.

increases as θ_γ increases, while that for the $j_<(p_{1/2})$ decreases.

As for the γ_c, the 3^- state is not a simple 1p-1h configuration, but it has rather complicated configurations. In fact an appreciable $d_{5/2} \rightarrow d_{3/2}$ $M1$ admixture into the $f_{7/2} \rightarrow d_{5/2}$ $E1$ has been reported at a lower proton energy.[2] Thus, interpretation of the γ_c data is not straightforward.

The strong peak γ_d feeding the 18.8 ± 0.5 MeV region may correspond to the big γ peak feeding the 19.2 ± 0.6 MeV state in Ref. 10. The broad peak γ_e feeding the 22.3 ± 1.0 MeV region has shown up for the first time in the present spectrum. The angular distributions of the cross sections for the γ_d and γ_e are similar to each other. It is interesting to note the sharp contrast of the observed analyzing powers for the γ_d and γ_e (Fig. 3). The effect of tails of higher energy γ rays is small, and cannot explain this large difference of the analyzing powers. Let us consider microscopic configurations of the excitation energy region of γ_d and γ_e. Using a simple direct model for the radiative proton capture reaction on ^{11}B with the $(p_{3/2})^{-1}$ configuration, the final states are mainly of 1-particle 1-$p_{3/2}$ hole states. The particle-hole configuration in the 18–23 MeV region has been studied by (e,e'),[20,21] (p,p'),[22] (α,α'),[22] and $(^3He,d)$ (Ref. 23) reactions and RPA calculations.[17–19] The $(J^\pi,T)=(2^-,1)$, $(3^-,1)$, $(4^-,1)$, and $(4^-,0)$ states with mainly the $(d_{5/2})(p_{3/2})^{-1}$ configuration are located in the 18.3–19.6 MeV excitation region of γ_d. The $[(d_{5/2})(p_{3/2})^{-1}]_{4^-}$ configuration is the most probable configuration of the 19.2 ± 0.6 MeV region.[10] On the other hand, the 20.6–22.5 MeV excitation region of γ_e includes the $(3^-,0)$, $(3^-,1)$, $(2^-,0)$, and $(2^-,1)$ states with mainly the $(d_{3/2})(p_{3/2})^{-1}$ configuration as well as the $(1^-,1)$ state with the $(d_{5/2})(p_{3/2})^{-1}$. Thus, the different features of the analyzing powers for the γ_d and γ_e may reflect, respectively, the $d_{5/2}$ and $d_{3/2}$ configurations of the final orbits. It is interesting to find that the observed analyzing powers for the γ_d and γ_e feeding unbound states show a similar j dependence as the observed tendency for the γ_a and γ_b feeding bound states. The analyzing powers for the γ_a and γ_d, which feed mainly the $j_> = l + \frac{1}{2}$ states, behave similarly as a function of the detection angle, while the γ_b and γ_e, which feed mainly the $j_< = l - \frac{1}{2}$ states, are also similar (see Fig. 3).

The present γ-ray energy region of 40–60 MeV clearly exceeds the $E1$ GR energy and is still far below the pion threshold. Thus, the major process is considered to be the direct process with mainly electric radiations. A simple direct model should be useful for comparing qualitatively with the data. The uniform forward peaking pattern of the angular distribution is explained by the stretched $E1$ radiation with an $E2$ admixture of the order of 10% in strength. The stretched electric radiation means that the incident wave contributing to the radiative capture into the $j_> = l_f + \frac{1}{2}$ orbit is mainly the $j_> = l_i + \frac{1}{2}$ proton and that to the $j_< = l_f - \frac{1}{2}$ is the $j_< = l_i - \frac{1}{2}$ one. The analyzing powers of the γ rays are explained qualitatively by the interference between a $j+1 \rightarrow j$ $E1$ radiation and a $j-1 \rightarrow j$ $E1$ radiation. The analyzing power evaluated by a simple direct model is really dependent on whether the final configuration is the $j_>$ or $j_<$. This feature is just what is observed. The semidirect (SD) process through the $E1$ GR, which is neglected in a simple direct model, is evaluated to be less than 20% at the 40 MeV γ-ray energy region on the basis of the Lorentzian form of the $E1$ GR with E_γ (GR) = 23 MeV.[9] In case of the SD process, the incident proton (j_i) excites first the $E1$ GR while it goes to the final (j_f) orbit through the $E1$-type nuclear interaction, being followed by the γ decay of the $E1$ GR. Because this $E1$-type nuclear process is similar to the direct $E1$ radiative process, the similar argument of the analyzing power holds even in the SD process. In fact, similar features were observed in the GR region.[3]

In short, the present work reports angular distributions and analyzing powers for medium energy (40–65 MeV) γ rays following interaction of medium energy (50 MeV) polarized protons. The newly developed HERMES showed good energy resolution, and a good separation of γ-ray signal from the background of neutrons and cosmic rays made it possible in practice to observe isolated γ rays associated with radiative captures into orbits with mainly the $p_{1/2}$, $p_{3/2}$, $d_{3/2}$, and $d_{5/2}$ configurations. The angular distributions of these γ rays all show similar forward peaking patterns, while the analyzing powers depend on the final orbits of $j_> = I + \frac{1}{2}$ and $j_< = I - \frac{1}{2}$. It was experimentally shown that the analyzing power of medium energy γ rays associated with the interaction of polarized protons is indeed a good probe to study the reaction mechanism and the microscopic

configuration of excited states. The medium energy γ radiation far beyond the GR is considered to be mainly due to the direct process[15,16,24] with appreciable contribution of the exchange current.[16,25] Extensive studies of such energetic polarized protons are interesting to clarify the possible contributions of the exchange currents.

The authors thank Mr. I. Sugai of the Institute for Nuclear Studies for preparation of the ^{11}B target, and Professor H. Kitazawa for the theoretical discussion. Many thanks are also due to the Research Center for Nuclear Physics cyclotron crew for the cyclotron operation under the program number 14A16.

---

*Present address: Physikalisches Institut der Universität Heidelberg, Heidelberg, Germany.
†Present address: Shimadzu Corporation, Kyoto, Japan.

[1]G. E. Brown, Nucl. Phys. **57**, 339 (1964).
[2]C. Brassard *et al.*, Phys. Rev. C **6**, 53 (1972).
[3]H. F. Glavish *et al.*, Phys. Rev. Lett. **28**, 766 (1972).
[4]K. A. Snover, P. Paul, and H. M. Kuan, Nucl. Phys. **A285**, 189 (1977).
[5]S. Manglos *et al.*, Phys. Rev. C **24**, 2378 (1981).
[6]F. Saporetti and R. Guidotti, Nucl. Phys. **A330**, 53 (1979).
[7]H. R. Weller *et al.*, Phys. Rev. C **25**, 2921 (1982).
[8]D. H. Dowell *et al.*, Phys. Rev. Lett. **50**, 1191 (1983).
[9]J. T. Londergan and L. D. Ludeking, Phys. Rev. C **25**, 1722 (1982).
[10]M. A. Kovash, S. L. Blatt, R. N. Boyd, T. R. Donoghue, H. J. Hausman, and A. D. Bacher, Phys. Rev. Lett. **42**, 700 (1979).
[11]M. Anghinolfi *et al.*, Nucl. Phys. **A399**, 66 (1983).
[12]T. Kishimoto, T. Shibata, M. Sasao, M. Noumachi, and H. Ejiri, Nucl. Instrum. Methods **198**, 269 (1982).
[13]M. Noumachi, Ph.D. thesis, Osaka University, 1983 (unpublished); M. Nomachi, H. Ejiri, T. Shibata, K. Okada, T. Motobayashi, T. Kishimoto, and F. Ohtani, in Proceedings of the 1983 Research Center for Nuclear Physics International Symposium on Light Ion Reaction Mechanism, Osaka, 1983, edited by H. Ogata, T. Kammuri, and I. Katayama (1984), p. 870.
[14]M. Nomachi *et al.*, in Proceedings of the International Symposium on Electromagnetic Properties of Atomic Nuclei, Tokyo, 1983, edited by H. Horie and H. Ohnuma (1984), p. 451.
[15]S. F. Tsai and J. T. Londergan, Phys. Rev. Lett. **43**, 576 (1979).
[16]M. Gari and H. Hebach, Phys. Rev. C **18**, 1071 (1978).
[17]V. Gillet and N. Vinh Mau, Nucl. Phys. **54**, 321 (1964).
[18]T. W. Donnelly, Phys. Rev. C **1**, 833 (1970).
[19]D. J. Rowe and S. S. M. Wong, Nucl. Phys. **A153**, 561 (1970).
[20]A. Yamaguchi, T. Terasawa, K. Nakahara, and Y. Torizuka, Phys. Rev. C **3**, 1750 (1971).
[21]T. W. Donnelly *et al.*, Phys. Rev. Lett. **21**, 1196 (1968); Ann. Phys. (N.Y.) **60**, 209 (1970).
[22]M. Buenerd, P. Martin, P. de Saintignon, and J. M. Loiseaux, Nucl. Phys. **A286**, 377 (1977).
[23]G. M. Reynolds, D. E. Rundquist, and R. M. Poichar, Phys. Rev. C **3**, 442 (1971).
[24]L. G. Arnold, Phys. Rev. Lett. **42**, 1253 (1979).
[25]H. Hebach, A. Wortberg, and M. Gari, Nucl. Phys. **A267**, 425 (1976); M. Gari and H. Hebach, Phys. Lett. **49B**, 29 (1974).